

## Phenological response of different vegetation types to temperature and precipitation variations in northern China during 1982–2012

Zexing Tao, Huanjiong Wang, Yachen Liu, Yunjia Xu & Junhu Dai

To cite this article: Zexing Tao, Huanjiong Wang, Yachen Liu, Yunjia Xu & Junhu Dai (2017) Phenological response of different vegetation types to temperature and precipitation variations in northern China during 1982–2012, International Journal of Remote Sensing, 38:11, 3236–3252, DOI: [10.1080/01431161.2017.1292070](https://doi.org/10.1080/01431161.2017.1292070)

To link to this article: <https://doi.org/10.1080/01431161.2017.1292070>



Published online: 24 Mar 2017.



Submit your article to this journal [↗](#)



Article views: 234



View related articles [↗](#)



View Crossmark data [↗](#)



Citing articles: 17 View citing articles [↗](#)



# Phenological response of different vegetation types to temperature and precipitation variations in northern China during 1982–2012

Zexing Tao <sup>a,b</sup>, Huanjiong Wang <sup>a</sup>, Yachen Liu <sup>a,c</sup>, Yunjia Xu <sup>a,b</sup>  
and Junhu Dai <sup>a</sup>

<sup>a</sup>Key Laboratory of Land Surface Pattern and Simulation, Institute of Geographic Sciences and Natural Resources Research, Chinese Academy of Sciences, Beijing, China; <sup>b</sup>University of Chinese Academy of Sciences, Beijing, China; <sup>c</sup>School of Geography, Beijing Normal University, Beijing, China

## ABSTRACT

Plant phenology is influenced by various climatic factors such as temperature, precipitation, insolation, and humidity, etc. Among these factors, temperature and precipitation are proved to be the most important. However, the relative importance of these two factors is different among various phenophases and regions and is seldom discussed along environmental gradients. Based on normalized difference vegetation index (NDVI) data from the NDVI3g dataset and using the mid-point method, we extracted the start date of the growing season (SOG) and the end date of the growing season (EOG) in northern China during 1982–2012. To determine which climate factor was more influential on plant phenology, partial correlation analysis was applied to analyse the spatial difference between the response of SOG and EOG to temperature and precipitation. Finally, we calculated the temperature and precipitation sensitivities of the SOG and EOG. The results showed that: (1) SOG displayed an advancing trend in most regions, while EOG was delayed for all the vegetation types during 1982–2012. (2) SOG was mainly triggered by pre-season temperature. The increase in temperature caused an overall advance in SOG. However, the relationship between SOG and precipitation varied among different vegetation types. Regarding EOG, precipitation had greater impacts than temperature in relatively arid environments, such as deserts, steppes and meadow biomes. (3) The response of vegetation phenology (both SOG and EOG) to temperature became stronger with increasing pre-season precipitation across space. The response of EOG to precipitation became weaker from arid regions to relatively humid regions. These results provide a better understanding of the spatial pattern of the phenological response along the precipitation gradient and a reference for assessing impacts of future climate change on vegetation phenology, especially in transitional and fragile zones.

## ARTICLE HISTORY

Received 21 April 2016  
Accepted 27 January 2017

## KEYWORDS

Phenology; growing season; remote sensing; climate change

## 1. Introduction

Robust changes in the climate system since the nineteenth century are unequivocal. In addition to the continuous increase of global warming, precipitation also increased with high confidence in the mid-latitude land areas of the Northern Hemisphere (IPCC 2013). These changes significantly influenced the vegetation growth of the terrestrial ecosystem in terms of both timing and duration.

Plant phenology has been widely used to indicate the impacts of climate change on biological systems (Linkosalo, Hakkinen, and Hanninen 2006; Gallagher, Hughes, and Leishman 2009; Chuine et al. 2004). Through various remote-sensing-based greenness indices, such as the normalized difference vegetation index (NDVI), two key phenological phases, the start of growing season (SOG) and the end of growing season (EOG), could be estimated. Therefore, remote-sensing data were widely used to monitor and characterize the temporal-spatial patterns of phenological changes and to analyse their relation to climate factors at large spatial scales (Chen et al. 2000; Forkel et al. 2015; He et al. 2015; Horion et al. 2013; Yang et al. 2012).

Previous findings revealed that the advanced spring phenology in middle and high latitudes was primarily triggered by climate warming (Wolfe et al. 2005; Menzel et al. 2006; Ge et al. 2015; Dai, Wang, and Ge 2013). However, the importance of temperature impact on phenology was considered to be somewhat overestimated (Forkel et al. 2015; Wolkovich et al. 2012) because climate factors other than temperature (i.e. precipitation) also exerted profound effects on the spring vegetation phenology (Gómez-Mendoza et al. 2008; Fu et al. 2014). Several studies argued that the influence of precipitation on vegetation phenology was even greater than that of temperature in water-limited biomes, such as the arid desert (Yang et al. 2015a), alpine tundra (Piao et al. 2006), dry steppe (Zhu and Meng 2015) and Tibetan Plateau (Shen et al. 2015). Cong et al. (2013) found precipitation to be a significant regulator controlling the response of spring phenology to temperature change in temperate China. Richardson et al. (2013) suggested that phenological changes occur as a result of both precipitation and temperature in a subtropical desert, but different climate factors affected different growth periods of the plants. Although the above studies clarified that precipitation, in addition to temperature, had a large influence on vegetation phenology, fewer studies quantitatively compared the relative importance of temperature and precipitation on vegetation phenology among different vegetation types. In addition, the spatial pattern of phenological response to temperature along a precipitation gradient was unclear.

In this study, we used NDVI data to extract SOG and EOG in northern China and analysed their temporal-spatial changes for the period 1982–2012. Subsequently, we performed partial correlation analysis between the phenophases and the two climatic drivers (temperature and precipitation) for different vegetation types. Meanwhile, the sensitivity of vegetation phenology to climate factors was estimated. Our objectives were to investigate: (1) which climate factor was more important in determining the start and end of the growing season among different vegetation types, and (2) how did vegetation phenology respond to temperature along a precipitation gradient?

## 2. Data and method

### 2.1. Study area

Northern China, spanning from 92.7° to 135.1°E and 34.9°N to 53.6°N, was selected as the study area because it included diverse vegetation types distributed along temperature and precipitation gradients. Figures 1(a–c) show 12 vegetation types identified by a digitized 1:100,000,000 vegetation map of China (Zhang 2007). Within this region, temperature showed an approximate decreasing trend from south to north with a maximum difference of 30.8°C, and precipitation ranged from 427.5 mm in the southeast to 11.7 mm in the northwest (Figures 1(a–c)).

### 2.2. Phenological and meteorological data

The NDVI data from northern China during 1982–2012 were acquired from the NDVI3g dataset produced by the Global Inventory Modelling and Mapping Studies (GIMMS) group (Pinzon and Tucker 2014). The spatial resolution of NDVI3g was 8 km and the temporal resolution was 15 days. This dataset had been proved to be effective for studying long-term variations in vegetation activities (Piao et al. 2006; Jeong et al. 2011; Wu and Liu 2013; Ghazaryan et al. 2016; Tsai, Lin, and Yang 2016).

In order to avoid the impact of land-use change on results of phenological changes, we also obtained land cover data of two periods (1980 and 2010) from Data Centre for Resources and Environmental Sciences (RESDC) of the Chinese Academy of Sciences. The spatial resolution of land cover data was 1 km. In this dataset, land-use types were divided into six categories, including forest, grassland, water, urban area, cultivated land, rural settlement, and barren land (Jiang et al. 2014).

The meteorological data were derived from the China Meteorological Forcing Dataset (He and Yang 2011). The dataset covered the period 1982–2012 with the spatial

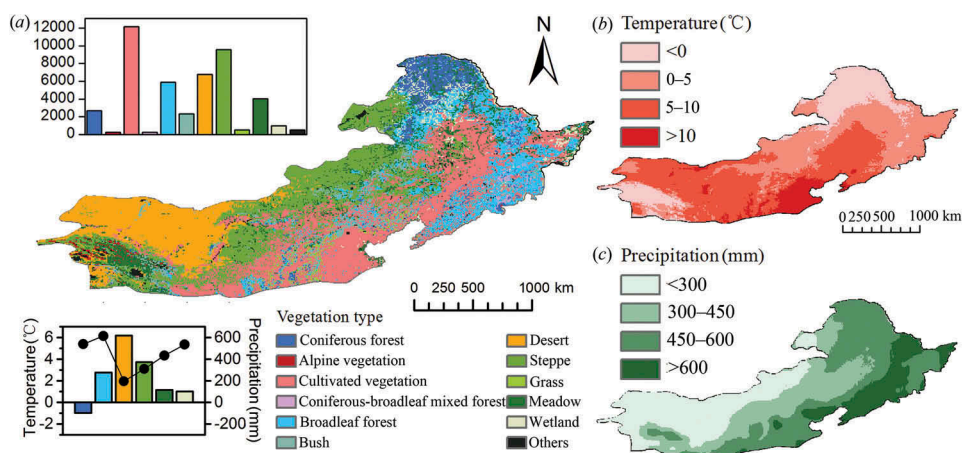


**Figure 1.** Vegetation types (a), annual mean temperature (b), and cumulative precipitation (c) during 1982–2012 in northern China. The histogram at upper left represents the numbers of pixels for different vegetation types. The map at bottom left shows the annual mean temperature (histograms) and cumulative precipitation (dots) for six main vegetation types.

resolution of  $0.1^\circ$  and temporal resolution of 3 h. In the study, the mean temperature and accumulated precipitation during the two months before the phenological date (mean SOG or EOG) was calculated for further analysis (Sakkir et al. 2015).

### 2.3. Method

Many methods had been used in determining the phenophases from satellite-derived NDVI data. However, phenological variations estimated by multiple methods showed large deviations even for the same region and period (Cong et al. 2013). Thus, the accuracy of different methods for specific regions required to be assessed by comparing the extracted phenophases with *in situ* observations (Nagai et al. 2010; White et al. 2009). In China's temperate monsoon area, the start of growing season calculated by Midpoint method exhibited the most significant correlations with ground observations compared with other methods (Wang et al. 2014a). Therefore, we applied the midpoint method to extract the SOG and EOG from the satellite-observed NDVI3g dataset for each pixel in this study.

Before extracting the phenophases, we first eliminated the highest and lowest 5% of NDVI values, which were probably aberrant value, in every annual NDVI series. Second, a cubic spline was applied to interpolate the NDVI series from 15 days to 1 day (White et al. 2009; Cong et al. 2013; Garonna et al. 2014). Finally, for every pixel, we computed the median NDVI series during 1982–2012. The midpoint of this NDVI series was used as a threshold to identify the SOG and EOG.

For all the pixels, the median NDVI series should meet the following criteria:

- (1) The annual mean NDVI of pixels must be greater than 0.1 and the annual maximum NDVI must be greater than 0.15 because pixels with low NDVI were likely to reflect the information of the soil background or other surface material rather than information about the vegetation (Zhou et al. 2003).
- (2) The vegetation types identified were natural vegetation. The phenology in cultivated regions was highly influenced by human activities, such as irrigation and fertilization.
- (3) The maximum NDVI occurred in June–September; NDVI in July–August should be greater than 1.35 times the NDVI in November–December and January–February. This could exclude the pixels with lack of vegetation seasonality, such as subtropical evergreen broadleaf forest (Shen et al. 2011). Meanwhile, the vegetation lack of seasonality was mostly located in areas with high precipitation, where the data are highly contaminated by clouds.

Subsequently, we removed outliers of the extracted SOG and EOG. For every pixel, we performed linear regression analysis between SOG or EOG and the year. The SOG and EOG in each year with residuals of more than 30 days were eliminated and replaced by the mean value from 1982 to 2012. If one pixel had more than 5 years of values removed, this pixel would not be considered in the following analyses.

Finally, we removed pixels with dramatic land cover changes from 1980 to 2010. To keep consistent with the resolution of NDVI data, land-use data was resampled from 1 to 8 km. The land cover information for each pixel was presented by the proportion of each land cover type (e.g. 50% steppe, 30% forest, and 20% desert). If one land cover type

occupied the maximum proportion within one pixel, we determined this type as the major land cover type of this pixel. Subsequently, we calculated the changes in percentages of major land cover type for each pixel from 1980 to 2010. The pixels whose difference in percentage between 1980 and 2010 was more than 15% would be removed from further analysis.

Through the above processes, the remaining number of pixels was 17,500. Most of these belonged to six vegetation types, including steppe (6485 pixels), broadleaf forest (3858 pixels), meadow (2349 pixels), coniferous forest (1470 pixels), wetland (489 pixels), and desert (717 pixels). The other 2132 pixels belonged to other vegetation types.

The trends of SOG and EOG were calculated by linear regression between phenophases and year. Subsequently, partial correlation between phenophases and temperature controlling precipitation was performed to analyse the relationships between the phenophases and temperature. Similarly, partial correlation between the phenophases and precipitation controlling temperature was performed. For pixels whose partial correlation coefficients ( $r$ ) were significant ( $p < 0.05$ ), the absolute value of  $r$  between phenophases and temperature was compared with that between phenophases and precipitation to examine which climate factor was more dominant in influencing vegetation phenology. Finally, temperature and precipitation sensitivity of the SOG and EOG were calculated to measure the degrees of phenological responses through linear regression between phenophases and preseason climate factors. The length of preseason was chosen to be two months before mean SOG or EOG following previous studies (Sakkir et al. 2015; Cong et al. 2013; Wang et al. 2014b, 2014c). If the mean SOG and EOG were in the first half of the month, the preseason was referred to the preceding two months, while if the phenophases occurred in the second half of the month, the preseason was referred to the previous and current month (Ge et al. 2016).

As our study area was quite large, it was essential to consider the effects of projection on the variation of pixel sizes along the latitudinal gradient. Therefore, mean phenophases or phenological trends were computed as the weighted average according to following equations:

$$a_i = \cos(L_i) \times \cos(L_i + S), \quad (1)$$

$$P_{\text{weighted}} = \frac{\sum_{i=1}^n (a_i \times P_i)}{\sum_{i=1}^n a_i}, \quad (2)$$

where  $a_i$  was the weight of each pixel  $i$ ;  $L_i$  was the latitude of pixel;  $S$  was the cell size;  $P_i$  represented the phenophases, phenological trend, or sensitivity to climate of pixel  $i$ ;  $n$  was the total number of pixels and  $P_{\text{weighted}}$  indicated the weighted average value.

### 3. Results

#### 3.1. Phenological trend (1982–2012)

The trends in SOG and EOG from 1982 to 2012 were shown in Figures 2(a–d). The changing trends in SOG and EOG varied among different pixels, both in sign and magnitude. Overall, 62.8% of the pixels showed an earlier shift in SOG by an average

rate of  $-1.57$  days decade $^{-1}$ , and 73.0% of the pixels showed a delaying trend of 1.48 days decade $^{-1}$  in EOG, on average. However, the trends of SOG and EOG were only significant ( $p < 0.05$ ) in 26.8% and 27.5% of the pixels, respectively. For 70.2% and 73.4% of pixels, the absolute value of trends in SOG and EOG was less than 1.00 days decade $^{-1}$  during the study period.

The interannual variations of SOG and EOG for six vegetation types are shown in Figures 3(a–l). The amplitudes of the variations in mean SOG time series ranged from 4.6 days in desert to 7.3 days in wetland with an average of 5.4 days. Significant advancing trends ( $p < 0.01$ ) were found for broadleaf forest ( $-0.8$  days decade $^{-1}$ ), meadow ( $-0.6$  days decade $^{-1}$ ), and wetland ( $-1.4$  days decade $^{-1}$ ). According to the standard deviations (SD) of SOG across all pixels, we found that SOG had stronger spatial variability in arid and semi-arid regions (SD: 11.6 days in desert, 10.1 days in steppe) than humid regions, such as forests (SD: 7.5 days in coniferous forest, 8.3 days in broadleaf forest) and wetland (SD: 7.9 days). EOG of all the vegetation types except wetland showed significant delaying trends. The amplitudes of the variations ranged from 4.1 days in coniferous forest and desert to 6.7 days in wetland with an average of 5.1 days. The SD of EOG across space for desert (4.0 days) and steppe (4.0 days) was smaller than that for meadow (4.3 days) and broadleaf forest (4.2 days).

### 3.2. Phenological response to temperature and precipitation

#### 3.2.1. Correlation between phenophases and pre-season temperature and precipitation

Figures 4(a–h) show the responses of SOG and EOG to temperature and precipitation change. The SOG was negatively correlated with temperature in 77.8% of the pixels and correlated with precipitation in 60.1% of the pixels, suggesting that the increase in

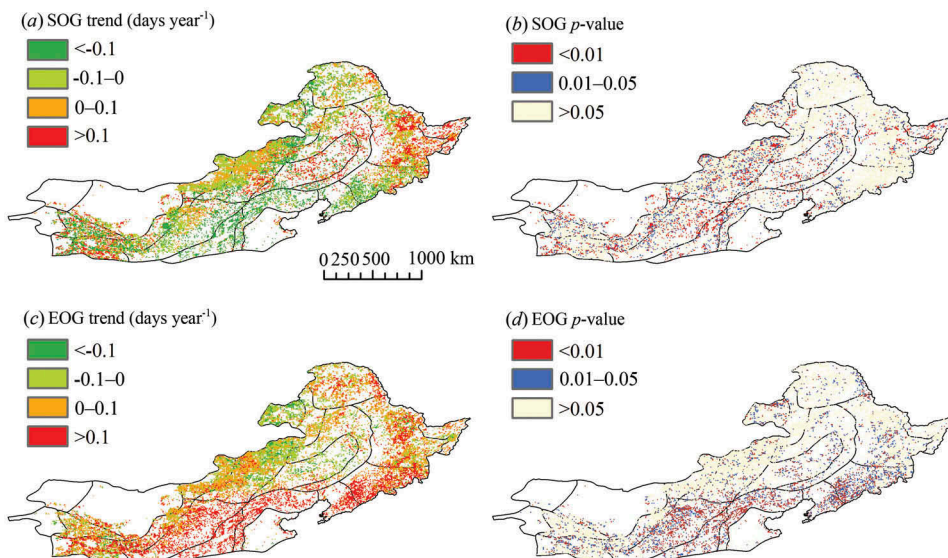


**Figure 2.** (a–d) Spatial distributions of trends in SOG and EOG during 1982–2012. SOG trend and EOG trend represent the trends of start of growing days and end of growing days, respectively. The  $p$ -value indicates the significant level of the trends in pixels.



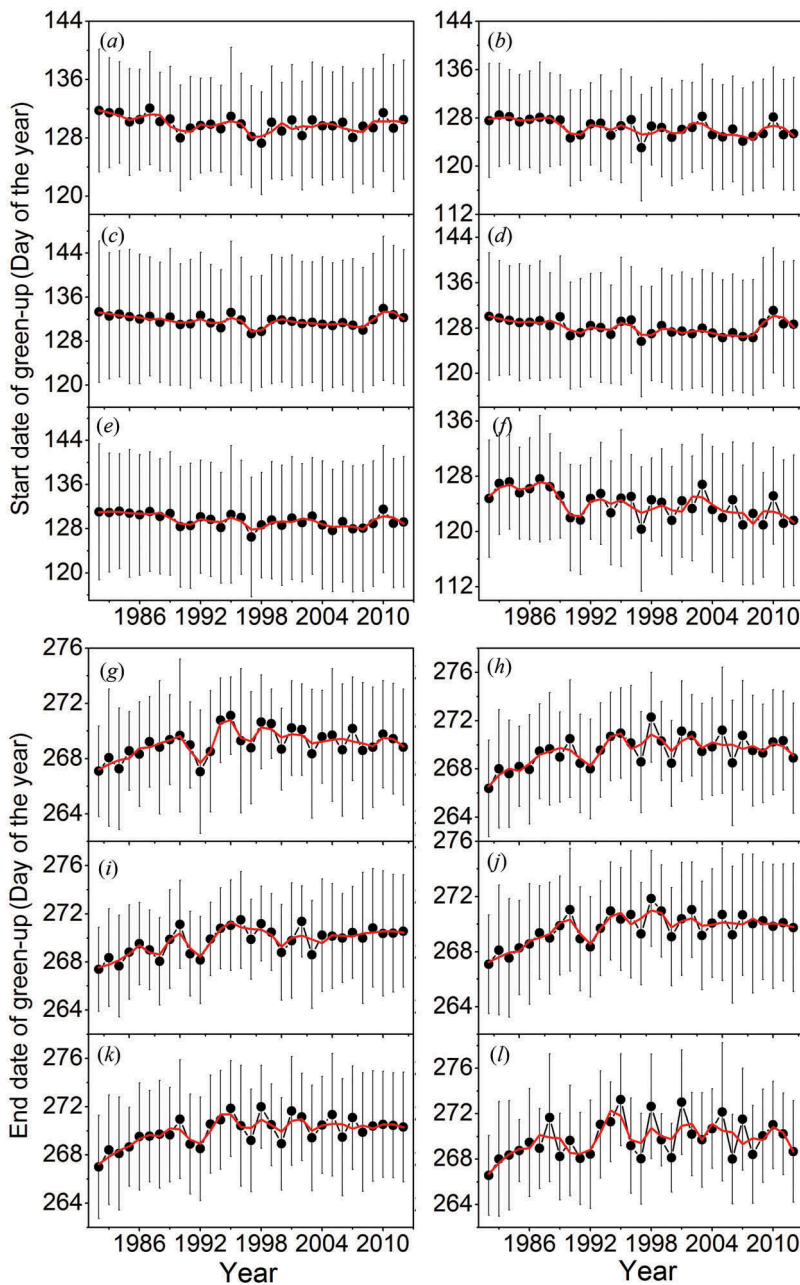


**Figure 3.** Inter-annual variations of the mean SOG (a–f) and EOG (g–l) for (a, g) coniferous forest, (b, h) broadleaf forest, (c, i) desert, (d, j) meadow, (e, k) steppe, (f, l) wetland in northern China during 1982–2012. Red lines indicate 5 year moving averages. Vertical lines are the spatial standard deviations among pixels.

temperature or precipitation would cause the SOG to advance. The  $p$ -values of the  $r$  revealed that the SOG was significantly correlated with temperature in 20.2% of the pixels ( $p < 0.05$ ), but only 6.9% of the pixels showed a significant correlation between the SOG and precipitation ( $p < 0.05$ ). Conversely, the EOG showed a positive correlation with temperature



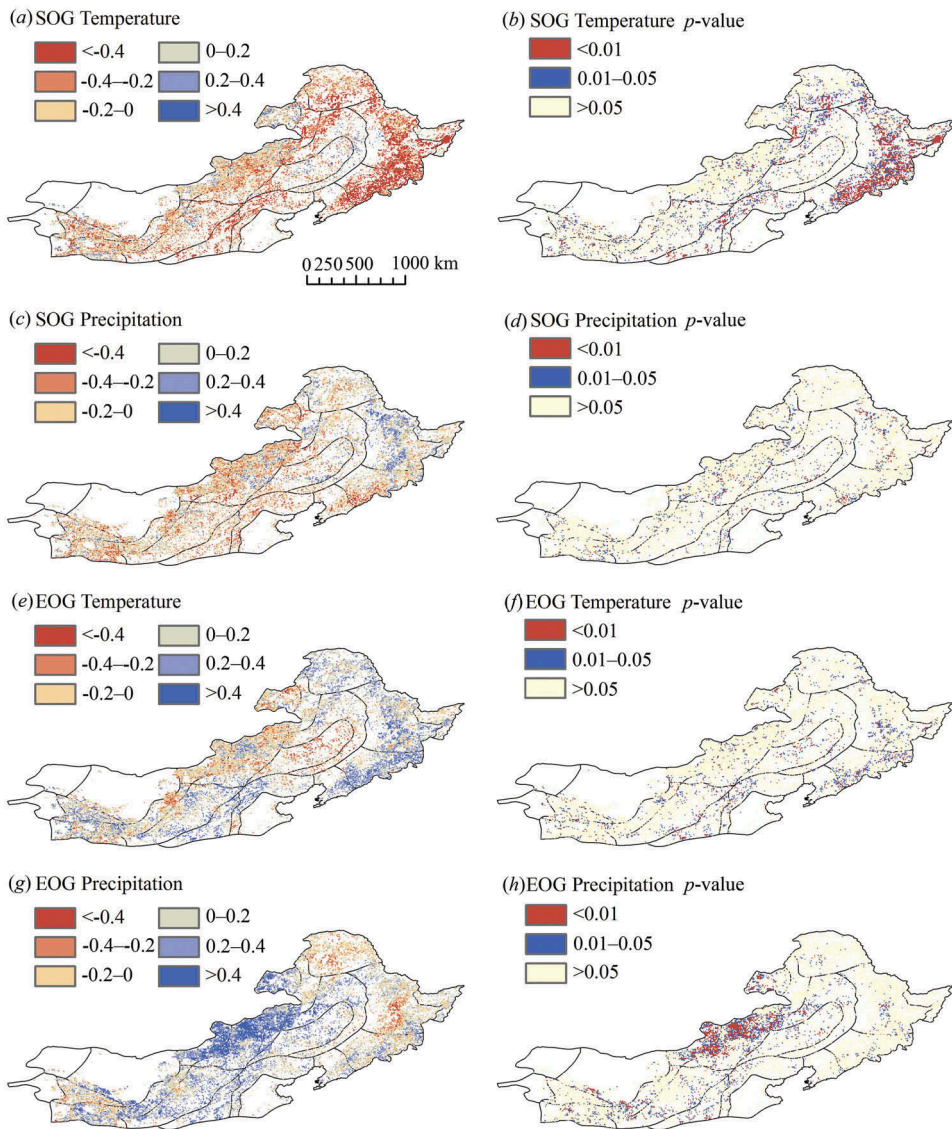


**Figure 4.** Spatial distributions of  $r$  between SOG and (a) temperature, (c) precipitation as well as EOG and (e) temperature, (g) precipitation. The significance of the correlations are shown in (b), (d), (f), and (h) in the same order.

in 64.7% of the pixels, but few  $r$  were significant. The EOG was found to be positively correlated with precipitation in 73.3% of the pixels, especially in temperate grassland (mid-north of the study area) where the  $r$  were significant ( $p < 0.05$ ).

On average, SOG was negatively correlated with temperature for all vegetation types (Table 1). The correlations for 65.2% of the pixels of broadleaf forest and 38.3% of the pixels of wetland were statistically significant ( $p < 0.05$ ), but the proportion of significant correlations was lower for desert (16.4%) and steppe (16.3%). Negative correlations between the SOG and precipitation were found in desert, steppe and meadow, but only 7.9% to 11.3% of the pixels were significant ( $p < 0.05$ ). Furthermore, EOG exhibited

**Table 1.** Mean partial correlation coefficients ( $r$ ) between the phenophases and the climatic factors for six vegetation types.

		Coniferous forest	Broadleaf forest	Desert	Steppe	Meadow	Wetland
SOG-temperature	$r$	-0.28	-0.40	-0.09	-0.11	-0.16	-0.26
	$p < 0.05$ (%)	36.49	65.23	16.36	16.34	25.85	38.35
SOG-precipitation	$r$	0.01	0.01	-0.08	-0.10	-0.02	0.02
	$p < 0.05$ (%)	5.12	10.36	7.86	11.26	9.43	5.36
EOG-temperature	$r$	0.16	0.20	0.05	0.00	0.07	0.09
	$p < 0.05$ (%)	10.62	19.83	6.94	7.90	9.71	4.23
EOG-precipitation	$r$	-0.02	0.07	0.26	0.30	0.13	0.05
	$p < 0.05$ (%)	7.03	8.98	38.67	40.34	16.96	7.42

$p < 0.05$ (%) shows the percentage of pixels with significant  $r$  at the 0.05 level for specific vegetation type. SOG and EOG indicate the start and end of growing season, respectively. SOG (EOG)-temperature is the partial correlation between phenophases (SOG or EOG) and temperature controlling precipitation, and SOG (EOG)-precipitation is the partial correlation between phenophases (SOG or EOG) and precipitation controlling temperature.

positive correlation with temperature for all vegetation types, and the percentage of pixels showing significant correlations ranged from 4.2% to 19.8%. The  $r$  between the EOG and precipitation were negative for coniferous forest but positive for the other five vegetation types. The significant correlations ( $p < 0.05$ ) were mainly concentrated in desert (38.7%) and steppe (40.3%).

**3.2.2. Main impact factor of phenological changes**

To determine the main driving factors of SOG and EOG across space, we compared the absolute value of the  $r$  of temperature and precipitation for each pixel (Figures 5(a,b)). The

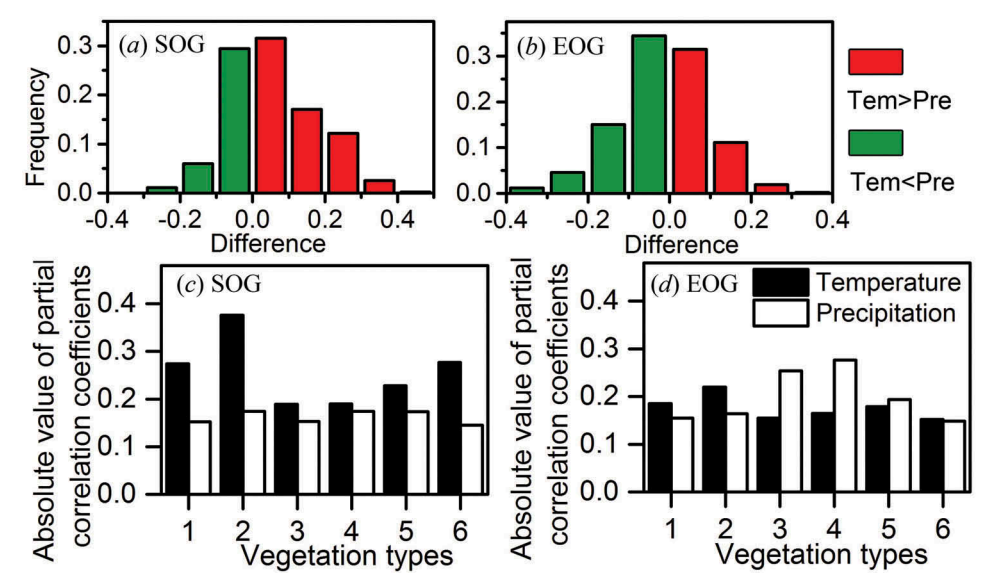


**Figure 5.** (a–d) Comparison of  $r$  between climate factors (temperature and precipitation) and phenophases (SOG and EOG). The difference was calculated between the absolute value of  $r$  between temperature and phenophases and the absolute value of  $r$  between precipitation and phenophases. Only the significant correlations were compared. The abbreviations ‘Tem’ and ‘Pre’ stand for temperature and precipitation, respectively. Numbers in x-axis in (c) and (d): 1: coniferous forest, 2: broadleaf forest, 3: desert, 4: meadow, 5: steppe, 6: wetland.

results indicate that SOG was highly correlated with temperature in most of the pixels (64.0%). For these pixels, the average preseason precipitation (13.7 mm) was greater than that for the remaining pixels (11.9 mm). Regarding EOG, precipitation was the main influencing factor in more than half of the pixels (54.8%). The preseason precipitation in these pixels was 42.5 mm on average, which was less than that of the other pixels (53.4 mm).

For all six vegetation types, SOG was more correlated with temperature (Figure 5(c)). The mean absolute values of the  $r$  between the SOG and temperature in forest and wetland were larger than those for desert and steppe. EOG was mainly influenced by preseason precipitation in desert, steppe and meadow (Figure 5(d)). For the EOG of coniferous forest, broadleaf forest and wetland, temperature was found to be the main influencing factor.

### 3.2.3. Phenological response to climate change along a precipitation gradient

Correlation analysis was applied to examine whether the  $r$  between the phenophases and temperature were related to precipitation across space. The phenological response (both SOG and EOG) to temperature became significantly stronger with increasing preseason precipitation (Figures 6(a,b)). Such a significant relationship was also robust

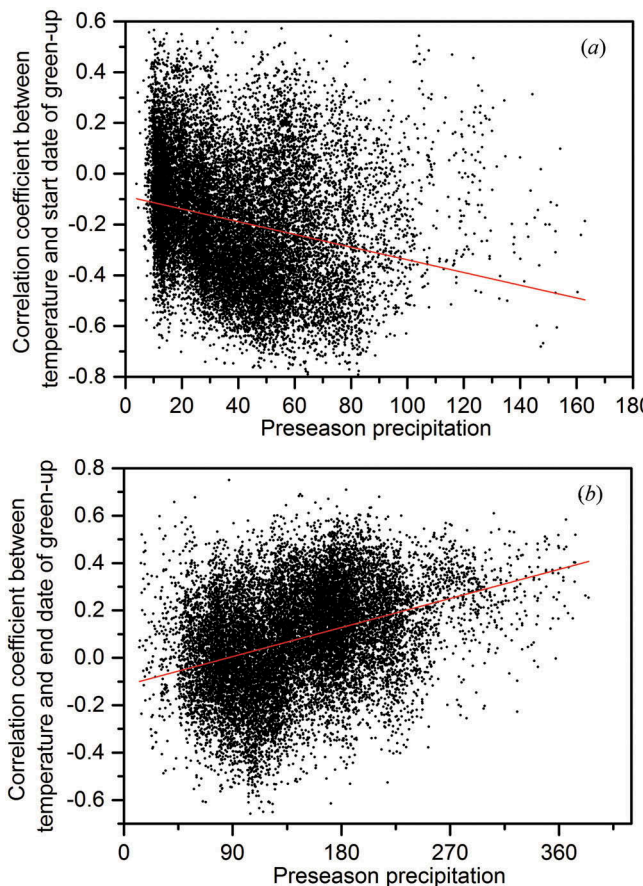


**Figure 6.** Phenological response to temperature along precipitation gradient. y-axis shows the  $r$  between phenophases and temperature (controlling precipitation). (a)  $y = -0.0025x - 0.089$  (Pearson's  $r = -0.23$ ,  $p < 0.01$ ); (b)  $y = 0.0014x - 0.12$  (Pearson's  $r = 0.36$ ,  $p < 0.01$ ).

**Table 2.** Pearson’s  $r$  between partial correlation coefficients and cumulative preseason precipitation for different vegetation types.

	Coniferous forest	Broadleaf forest	Desert	Steppe	Meadow	Wetland	Overall
SOG	−0.15**	−0.11**	−0.07**	−0.04**	−0.01**	−0.15**	−0.23**
EOG	0.1**	0.33**	0.07	0.16**	0.16**	0.02	0.36**

Partial correlation is performed between phenophases (SOG or EOG) and temperature controlling precipitation.  
\*\* $p < 0.01$ .

for each vegetation type, except for EOG and preseason precipitation in desert and wetland (Table 2).

### 3.3. Temperature and precipitation sensitivity of SOG and EOG

On average, the temperature and precipitation sensitivity of SOG was  $-0.67$  days/ $^{\circ}\text{C}$  and  $-1.37$  days/100 mm, respectively (Figures 7(a,c)). The temperature sensitivity of SOG in coniferous forest, broadleaf forest and wetland was much larger than in desert and steppe (Table 3). The precipitation sensitivity for the six vegetation types ranged from  $-2.87$  days/100 mm in steppe to 1.02 days/100 mm in wetland.

The average temperature and precipitation sensitivities of EOG were 0.25 days/ $^{\circ}\text{C}$  and 1.24 days/100 mm, respectively (Figures 7(b,d)). The temperature sensitivity showed evident spatial heterogeneity among different vegetation types. It reached 0.22–0.81 days/ $^{\circ}\text{C}$  on average for coniferous forest, broadleaf forest and wetland but was only  $-0.24$  days/ $^{\circ}\text{C}$  to  $-0.02$  days/ $^{\circ}\text{C}$  on average for desert and steppe. The precipitation sensitivity ranged from  $-0.23$  to 0.14 days/100 mm for coniferous forest, broadleaf forest and wetland, but the precipitation sensitivity of desert and steppe was stronger (2.24–3.32 days/100 mm).

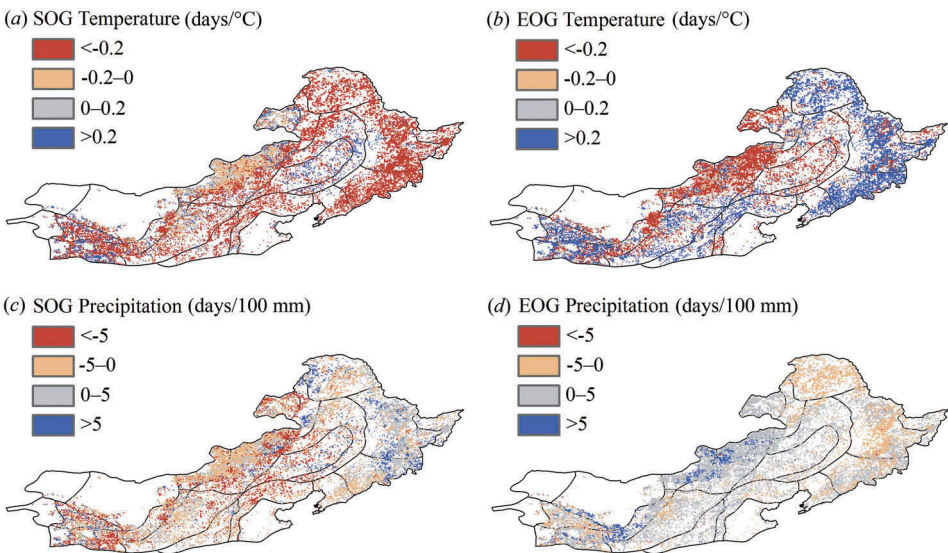


**Figure 7.** Spatial distributions of sensitivity of SOG to (a) temperature (days/ $^{\circ}\text{C}$ ) and (c) precipitation (days/100 mm) as well as sensitivity of EOG to (b) temperature (days/ $^{\circ}\text{C}$ ) and (d) precipitation (days/100 mm).

**Table 3.** Average temperature and precipitation sensitivities of the SOG and the EOG for each vegetation type.

	Coniferous forest	Broadleaf forest	Desert	Steppe	Meadow	Wetland
OG-Temperature (days/°C)	$-0.82 \pm 1.24$	$-1.11 \pm 1.24$	$-0.15 \pm 1.17$	$-0.34 \pm 1.36$	$-0.51 \pm 1.97$	$-0.76 \pm 1.79$
SOG-Precipitation (days/100 mm)	$0.96 \pm 8.43$	$0.68 \pm 6.68$	$-1.32 \pm 11.96$	$-2.87 \pm 9.71$	$-1.27 \pm 9.92$	$1.02 \pm 7.51$
EOG-Temperature (days/°C)	$0.73 \pm 1.95$	$0.81 \pm 1.80$	$-0.02 \pm 1.92$	$-0.24 \pm 1.36$	$0.17 \pm 1.35$	$0.22 \pm 1.47$
EOG-Precipitation (days/100 mm)	$-0.23 \pm 2.25$	$0.14 \pm 1.927$	$3.32 \pm 6.02$	$2.24 \pm 3.01$	$0.81 \pm 2.45$	$0.03 \pm 1.67$

The numbers after '±' represent the average 95% confidence intervals.

#### 4. Discussion

The average trend of spring phenology in northern China estimated in this study was  $-1.57$  days decade<sup>-1</sup>, which was in accordance with the result of Xu and Chen (2013) ( $-1.6$  to  $-1.4$  days decade<sup>-1</sup>), but a little larger than that estimated by Cong et al. (2013) based on the same method ( $-1.3$  days decade<sup>-1</sup>). Such differences could be explained by specific data processing procedure in this study. We considered the impact of land-use change on the results. The pixels with evident variations in vegetation types, which might consequently result in stronger advancing trend, were eliminated. In addition, we calculated the weighted average value, rather than the average value of SOG trend for all the pixels because the pixels sizes at lower latitudes was larger than those at higher latitudes. According to our analysis (Figures 2(a–d)), the advancing trend of SOG was greater at lower latitude. When computing the average trend, the contribution of pixels at higher latitude was enlarged, and this would lead to a smaller trend value. Similarly, the EOG trend in this study ( $1.48$  days decade<sup>-1</sup>) was also larger than other results (Liu et al. 2015).

Our results could also be compared with previous studies based on *in situ* observations. Ge et al. (2013) found a mean trend of  $-1.70$  days decade<sup>-1</sup> for spring phenophases in temperate China from 1963 to 2011, which was close to our result. However, in the study of Dai, Wang, and Ge (2013), the first leaf date in northern China showed a lower average advancing trend of  $-0.78$  days decade<sup>-1</sup>, and the trend in the study of Zang et al. (2011) reached  $-4.27$  days decade<sup>-1</sup>, which was almost three times as much as ours, in Shandong Province of China. The notable difference was mainly due to two reasons. First, different species and locations would lead to distinct estimates for ground phenology. The limited field observations and lack of community surveys in China might result in large discrepancies in estimating phenological trends. Moreover, significant spatiotemporal scale mismatch still existed between satellite-based land surface phenology and ground phenology (Wang et al. 2014a; Liang, Schwartz, and Fei 2011). The relationship of multi-scale phenology required further investigations.

Furthermore, we proved that the advance in spring phenology was majorly triggered by the rise of pre-season temperature, which was in accordance with previous findings (Wolfe et al. 2005; Menzel et al. 2006; Ge et al. 2015). Even in water-limited vegetation types (e.g. desert and steppe), temperature was suggested to be the most crucial influencing factor rather than precipitation, although a more important role of precipitation was expected in these regions (Yang et al. 2015a; Piao et al. 2006; Chen et al. 2014).

EOG was more correlated with the temperature than precipitation in coniferous forests, broadleaf forests and wetlands, as many other studies affirmed (Gill et al. 2015; Yang et al.



2015b). However, we doubted whether the preseason temperature alone was the primary impact factor on the autumn vegetation phenology in these vegetation types. In this study, the effect of precipitation was removed through partial correlation analysis when measuring the relationship between EOG and temperature. We noted that the proportion of significantly correlated pixels only ranged from 4.28% to 18.68%, which was notably smaller than the results calculated by the linear correlation method (Yang et al. 2015b), suggesting that the influence of preseason temperature on autumn phenology was regulated by precipitation. One assumption was that precipitation might affect the heat requirement of vegetation during dormancy, but this still needed to be verified further (Fu et al. 2015). Other factors, such as elevation of the CO<sub>2</sub> concentration, nitrogen addition, and incoming radiation, could also potentially interact with temperature to enhance or weaken the influence of temperature on autumn phenology (Forkel et al. 2015; Liu et al. 2015; Gill et al. 2015; Xia and Wan 2013). By contrast, the correlation between the EOG and preseason precipitation in the steppe and desert was significant in almost half of the pixels, demonstrating precipitation was the dominant factor influencing autumn phenology in arid and semi-arid vegetation types.

However, the effect of water condition on vegetation phenology in arid and semi-arid regions still requires more detailed study. On the one hand, available water was not only supplied by precipitation but was also associated with melt water from glaciers and permafrost soil, as well as underground water in specific regions (Forkel et al. 2015). On the other hand, the response of phenology to precipitation was recognized to be complex and varied in different time lags and durations (Gómez-Mendoza et al. 2008; Yang et al. 2015a).

In addition, we found the phenological response to temperature was positively and significantly correlated with preseason precipitation, which was consistent with other studies (Cong et al. 2013; Yang et al. 2015b). Considering that EOG was mainly triggered by preseason precipitation in arid and semi-arid regions such as desert and steppe, we could further analyse the response of EOG to precipitation along the precipitation gradient in these areas. The negative and significant correlation for desert and steppe (Pearson's  $r = -0.16$  and  $-0.27$ ,  $p < 0.01$ ) suggested that the importance of precipitation gradually decreased from arid regions to relatively humid regions.

## 5. Conclusions

In this study, we extracted the SOG and EOG of vegetation in northern China from satellite-based NDVI data, and estimated the phenological trends in different vegetation types during 1982–2012. Furthermore, the spatial patterns of the relationship between climate factors and phenophases were investigated. The conclusions were as follows:

- (1) SOG became earlier and EOG became later in most regions of northern China over the past three decades. However, the magnitude of trends was weak (less than 1.00 days decade<sup>-1</sup>) in more than 70% of pixels.
- (2) SOG was mainly triggered by preseason temperature for all the six vegetation types, and the rise in temperature caused advance in SOG. The  $r$  between the SOG and temperature for coniferous forest, broadleaf forest and wetland areas were much larger than that for desert and steppe. Regarding EOG, temperature was the



major influencing factor for coniferous and broadleaf forests, but precipitation might be a considerable regulator in desert and steppe areas.

- (3) Along the precipitation gradient from arid regions to relatively humid regions, the correlation between phenophases (both SOG and EOG) and temperature became significantly stronger. Meanwhile, the response of EOG to precipitation became weaker in more humid regions.

## Disclosure statement

No potential conflict of interest was reported by the authors.

## Funding

This work was supported by the National Program on Key Basic Research Project of China [grant number 2012CB955304]; National Natural Science Foundation of China [grant number 41427805; 41171043; 41601047]; National Natural Science Foundation of China [grant number 41171043]; and Strategic Priority Research Program of the Chinese Academy of Sciences [grant number XDA05090301].

## ORCID

Zexing Tao  <http://orcid.org/0000-0002-5276-5836>  
 Huanjiong Wang  <http://orcid.org/0000-0002-2325-0120>  
 Yachen Liu  <http://orcid.org/0000-0002-1164-6566>  
 Yunjia Xu  <http://orcid.org/0000-0002-7634-4147>  
 Junhu Dai  <http://orcid.org/0000-0001-6401-1735>

## References

- Chen, X., Z. J. Tan, M. D. Schwartz, and C. X. Xu. 2000. "Determining the Growing Season of Land Vegetation on the Basis of Plant Phenology and Satellite Data in Northern China." *International Journal of Biometeorology* 44 (2): 97–101. doi:10.1007/s004840000056.
- Chen, X. Q., J. Li, L. Xu, and D. Ding. 2014. "Modeling Greenup Date of Dominant Grass Species in the Inner Mongolian Grassland Using Air Temperature and Precipitation Data." *International Journal of Biometeorology* 58 (4): 463–471. doi:10.1007/s00484-013-0732-1.
- Chuine, I., P. Yiou, N. Viovy, B. Seguin, V. Daux, and E. L. R. Ladurie. 2004. "Historical Phenology: Grape Ripening as a Past Climate Indicator." *Nature* 432 (7015): 289–290. doi:10.1038/432289a.
- Cong, N., T. Wang, H. J. Nan, Y. C. Ma, X. H. Wang, R. B. Myneni, and S. L. Piao. 2013. "Changes in Satellite-Derived Spring Vegetation Green-Up Date and Its Linkage to Climate in China from 1982 to 2010: A Multimethod Analysis." *Global Change Biology* 19 (3): 881–891. doi:10.1111/gcb.12077.
- Dai, J. H., H. J. Wang, and Q. S. Ge. 2013. "Multiple Phenological Responses to Climate Change among 42 Plant Species in Xi'an, China." *International Journal of Biometeorology* 57 (5): 749–758. doi:10.1007/s00484-012-0602-2.
- Forkel, M., M. Migliavacca, K. Thonicke, M. Reichstein, S. Schaphoff, U. Weber, and N. Carvalhais. 2015. "Cot dominant Water Control on Global Interannual Variability and Trends in Land Surface Phenology and Greenness." *Global Change Biology* 21 (9): 3414–3435. doi:10.1111/gcb.12950.
- Fu, Y. H., S. Piao, Y. Vitasse, H. F. Zhao, H. J. D. Boeck, Q. Liu, H. Yang, U. Weber, H. Hänninen, and I. A. Janssens. 2015. "Increased Heat Requirement for Leaf Flushing in Temperate Woody Species

- over 1980–2012: Effects of Chilling, Precipitation and Insolation." *Global Change Biology* 21 (7): 2687–2697. doi:[10.1111/gcb.12863](https://doi.org/10.1111/gcb.12863).
- Fu, Y. H., S. L. Piao, H. F. Zhao, S. Jeong, X. H. Wang, Y. Vitasse, P. Ciais, and I. A. Janssens. 2014. "Unexpected Role of Winter Precipitation in Determining Heat Requirement for Spring Vegetation Green-Up at Northern Middle and High Latitudes." *Global Change Biology* 20 (12): 3743–3755. doi:[10.1111/gcb.12610](https://doi.org/10.1111/gcb.12610).
- Gallagher, R. V., L. Hughes, and M. R. Leishman. 2009. "Phenological Trends among Australian Alpine Species: Using Herbarium Records to Identify Climate-Change Indicators." *Australian Journal of Botany* 57 (1): 1–9. doi:[10.1071/BT08051](https://doi.org/10.1071/BT08051).
- Garonna, I., R. Dejong, A. J. W. Dewit, C. A. Mùcher, B. Schmid, and M. E. Schaepman. 2014. "Strong Contribution of Autumn Phenology to Changes in Satellite-Derived Growing Season Length Estimates across Europe (1982–2011)." *Global Change Biology* 20 (11): 3457–3470. doi:[10.1111/gcb.12625](https://doi.org/10.1111/gcb.12625).
- Ge, Q. S., J. H. Dai, H. J. Cui, and H. J. Wang. 2016. "Spatiotemporal Variability in Start and End of Growing Season in China Related to Climate Variability." *Remote Sensing* 8 (5): 1–16. doi:[10.3390/rs8050433](https://doi.org/10.3390/rs8050433).
- Ge, Q. S., H. J. Wang, and J. H. Dai. 2013. "Shifts In Spring Phenophases, Frost Events And Frost Risk For Woody Plants In Temperate China." *Climate Research* 57 (3): 249–258. doi:[10.3354/cr01182](https://doi.org/10.3354/cr01182).
- Ge, Q. S., H. J. Wang, T. Rutishauser, and J. H. Dai. 2015. "Phenological Response to Climate Change in China: A Meta-Analysis." *Global Change Biology* 21 (1): 265–274. doi:[10.1111/gcb.12648](https://doi.org/10.1111/gcb.12648).
- Ghazaryan, G., O. Dubovyk, N. Kussul, and G. Menz. 2016. "Towards an Improved Environmental Understanding of Land Surface Dynamics in Ukraine Based on Multi-Source Remote Sensing Time-Series Datasets from 1982 to 2013." *Remote Sensing* 8 (8): 1–16. doi:[10.3390/rs8080617](https://doi.org/10.3390/rs8080617).
- Gill, A. L., A. S. Gallinat, R. Sanders-DeMott, A. J. Rigden, D. J. Short-Gianotti, J. A. Mantooh, and P. H. Templer. 2015. "Changes in Autumn Senescence in Northern Hemisphere Deciduous Trees: A Meta-Analysis of Autumn Phenology Studies." *Annals of Botany* 116 (6): 875–888. doi:[10.1093/aob/mcv055](https://doi.org/10.1093/aob/mcv055).
- Gómez-Mendoza, L., L. Galicia, M. L. Cuevas-Fernández, V. Magaña, G. Gómez, and J. L. Palacio-Prieto. 2008. "Assessing Onset and Length of Greening Period in Six Vegetation Types in Oaxaca, Mexico, Using NDVI-Precipitation Relationships." *International Journal of Biometeorology* 52 (6): 511–520. doi:[10.1007/s00484-008-0147-6](https://doi.org/10.1007/s00484-008-0147-6).
- He, J., and K. Yang. 2011. *China Meteorological Forcing Dataset, Lanzhou, China: Science Data Center in Cold and Arid Regions*. doi:[10.3972/westdc.002.2014.db](https://doi.org/10.3972/westdc.002.2014.db).
- He, Z. B., J. Du, W. Zhao, J. J. Yang, L. F. Chen, X. Zhu, X. X. Chang, and H. Liu. 2015. "Assessing Temperature Sensitivity of Subalpine Shrub Phenology in Semi-Arid Mountain Regions of China." *Agricultural and Forest Meteorology* 213: 42–52. doi:[10.1016/j.agrformet.2015.06.013](https://doi.org/10.1016/j.agrformet.2015.06.013).
- Horion, S., Y. Cornet, M. Epicum, and B. Tychon. 2013. "Studying Interactions between Climate Variability and Vegetation Dynamic Using a Phenology Based Approach." *International Journal of Applied Earth Observation and Geoinformation* 20: 20–32. doi:[10.1016/j.jag.2011.12.010](https://doi.org/10.1016/j.jag.2011.12.010).
- IPCC. 2013. *Summary for Policymakers. Climate Change 2013. the Physical Science Basis. Contribution of Working Group I to the Fifth Assessment Report of the Intergovernmental Panel on Climate Change*, 1–1535. UK: Cambridge University Press.
- Jeong, S., C. Ho, H. Gim, and M. Brown. 2011. "Phenology Shifts at Start Vs. End of Growing Season in Temperate Vegetation over the Northern Hemisphere for the Period 1982–2008." *Global Change Biology* 17 (7): 2385–2399. doi:[10.1111/j.1365-2486.2011.02397.x](https://doi.org/10.1111/j.1365-2486.2011.02397.x).
- Jiang, D., M. Hao, D. Zhuang, and Y. Huang. 2014. "Spatial-Temporal Variation of Marginal Land Suitable for Energy Plants from 1990 to 2010 in China." *Scientific Report* 4 (5816): 1–8. doi:[10.1038/srep05816](https://doi.org/10.1038/srep05816).
- Liang, L., M. D. Schwartz, and S. Fei. 2011. "Validating Satellite Phenology through Intensive Ground Observation and Landscape Scaling in a Mixed Seasonal Forest." *Remote Sensing of Environment* 115 (1): 143–157. doi:[10.1016/j.rse.2010.08.013](https://doi.org/10.1016/j.rse.2010.08.013).
- Linkosalo, T., R. Hakkinen, and H. Hanninen. 2006. "Models of the Spring Phenology of Boreal and Temperate Trees: Is There Something Missing?" *Tree Physiology* 26 (9): 1165–1172. doi:[10.1093/treephys/26.9.1165](https://doi.org/10.1093/treephys/26.9.1165).

- Liu, Q., Y. H. Fu, Z. Z. Zeng, M. T. Huang, X. R. Li, and S. L. Piao. 2015. "Temperature, Precipitation, and Insolation Effects on Autumn Vegetation Phenology in Temperate China." *Global Change Biology* 22 (2): 644–655. doi:[10.1111/gcb.13081](https://doi.org/10.1111/gcb.13081).
- Menzel, A., T. H. Sparks, N. Estrella, E. Koch, A. Aasa, R. Ahas, K. Alm-Kübler, et al. 2006. "European Phenological Response to Climate Change Matches the Warming Pattern." *Global Change Biology* 12 (10): 1969–1976. doi:[10.1111/j.1365-2486.2006.01193.x](https://doi.org/10.1111/j.1365-2486.2006.01193.x).
- Nagai, S., K. N. Nasahara, H. Muraoka, T. Akiyama, and S. Tsuchida. 2010. "Field Experiments to Test the Use of the Normalized Difference Vegetation Index for Phenology Detection." *Agricultural and Forest Meteorology* 150 (2): 152–160. doi:[10.1016/j.agrformet.2009.09.010](https://doi.org/10.1016/j.agrformet.2009.09.010).
- Piao, S. L., J. Y. Fang, L. M. Zhou, P. Ciais, and B. Zhu. 2006. "Variations in Satellite-Derived Phenology in China's Temperate Vegetation." *Global Change Biology* 12 (4): 672–685. doi:[10.1111/j.1365-2486.2006.01123.x](https://doi.org/10.1111/j.1365-2486.2006.01123.x).
- Pinzon, J. E., and C. J. Tucker. 2014. "A Non-Stationary 1981–2012 AVHRR NDVI3g Time Series." *Remote Sensing* 6 (8): 6929–6960. doi:[10.3390/rs6086929](https://doi.org/10.3390/rs6086929).
- Richardson, A. D., T. F. Keenan, M. Migliavacca, Y. Ryu, O. Sonnentag, and M. Toomey. 2013. "Climate Change, Phenology, and Phenological Control of Vegetation Feedbacks to the Climate System." *Agricultural and Forest Meteorology* 169: 156–173. doi:[10.1016/j.agrformet.2012.09.012](https://doi.org/10.1016/j.agrformet.2012.09.012).
- Sakkir, S., J. N. Shah, A. J. Cheruth, and M. Kabshawi. 2015. "Phenology of Desert Plants from an Arid Gravel Plain in Eastern United Arab Emirates." *Journal of Arid Land* 7 (1): 54–62. doi:[10.1007/s40333-014-0036-2](https://doi.org/10.1007/s40333-014-0036-2).
- Shen, M. G., S. L. Piao, N. Cong, G. X. Zhang, and I. A. Jassens. 2015. "Precipitation Impacts on Vegetation Spring Phenology on the Tibetan Plateau." *Global Change Biology* 21 (10): 3647–3656. doi:[10.1111/gcb.12961](https://doi.org/10.1111/gcb.12961).
- Shen, M. G., Y. H. Tang, J. Chen, X. L. Zhu, and Y. H. Zheng. 2011. "Influences of Temperature and Precipitation before the Growing Season on Spring Phenology in Grasslands of the Central and Eastern Qinghai-Tibetan Plateau." *Agricultural and Forest Meteorology* 151 (12): 1711–1722. doi:[10.1016/j.agrformet.2011.07.003](https://doi.org/10.1016/j.agrformet.2011.07.003).
- Tsai, H. P., Y. Lin, and M. Yang. 2016. "Exploring Long Term Spatial Vegetation Trends in Taiwan from AVHRR NDVI3g Dataset Using RDA and HCA Analyses." *Remote Sensing* 8 (4): 1–20. doi:[10.3390/rs8040290](https://doi.org/10.3390/rs8040290).
- Wang, H. J., J. H. Dai, and Q. S. Ge. 2014a. "Comparison of Satellite and Ground-Based Phenology in China's Temperate Monsoon Area." *Advances in Meteorology* 2014: 1–10. doi:[10.1155/2014/474876](https://doi.org/10.1155/2014/474876).
- Wang, H. J., Q. S. Ge, J. H. Dai, and Z. X. Tao. 2014b. "Geographical Pattern in First Bloom Variability and Its Relation to Temperature Sensitivity in the USA and China." *International Journal of Biometeorology* 59 (8): 961–969. doi:[10.1007/s00484-014-0909-2](https://doi.org/10.1007/s00484-014-0909-2).
- Wang, T., C. Ottlé, S. Peng, I. A. Janssens, X. Lin, B. Poulter, C. Yue, and P. Ciais. 2014c. "The Influence of Local Spring Temperature Variance on Temperature Sensitivity of Spring Phenology." *Global Change Biology* 20 (5): 1473–1480. doi:[10.1111/gcb.12509](https://doi.org/10.1111/gcb.12509).
- White, M. A., K. M. de Beurs, K. Didan, D. W. Inouye, A. D. Richardson, O. P. Jensen, J. O'keefe, et al. 2009. "Intercomparison, Interpretation, and Assessment of Spring Phenology in North America Estimated from Remote Sensing for 1982–2006." *Global Change Biology* 15 (10): 2335–2359. doi:[10.1111/j.1365-2486.2009.01910.x](https://doi.org/10.1111/j.1365-2486.2009.01910.x).
- Wolfe, D. W., M. D. Schwartz, A. N. Lakso, Y. Otsuki, R. M. Pool, and N. J. Shaulis. 2005. "Climate Change and Shifts in Spring Phenology of Three Horticultural Woody Perennials in Northeastern USA." *International Journal of Biometeorology* 49 (5): 303–309. doi:[10.1007/s00484-004-0248-9](https://doi.org/10.1007/s00484-004-0248-9).
- Wolkovich, E. M., B. I. Cook, J. M. Allen, T. M. Crimmins, J. L. Betancourt, S. E. Travers, S. Pau, et al. 2012. "Warming Experiments Underpredict Plant Phenological Responses to Climate Change." *Nature* 485 (7399): 494–497. doi:[10.1038/nature11014](https://doi.org/10.1038/nature11014).
- Wu, X. C., and H. Y. Liu. 2013. "Consistent Shifts in Spring Vegetation Green-Up Date across Temperate Biomes in China, 1982–2006." *Global Change Biology* 19 (3): 870–880. doi:[10.1111/gcb.12086](https://doi.org/10.1111/gcb.12086).

- Xia, J., and S. Wan. 2013. "Independent Effects of Warming and Nitrogen Addition on Plant Phenology in the Inner Mongolian Steppe." *Annals of Botany* 111 (6): 1207–1217. doi:[10.1093/aob/mct079](https://doi.org/10.1093/aob/mct079).
- Xu, L., and X. Q. Chen. 2013. "Regional Unified Model-Based Leaf Unfolding Prediction from 1960 to 2009 across Northern China." *Global Change Biology* 19 (4): 1275–1284. doi:[10.1111/gcb.12095](https://doi.org/10.1111/gcb.12095).
- Yang, X., J. F. Mustard, J. W. Tang, and H. Xu. 2012. "Regional-Scale Phenology Modeling Based on Meteorological Records and Remote Sensing Observations." *Advances in Meteorology* 117: 1–18. doi:[10.1029/2012JG001977](https://doi.org/10.1029/2012JG001977).
- Yang, Y., C. Zhao, M. Han, Y. Li, and R. Yang. 2015a. "Temporal Patterns of Shrub Vegetation and Variation with Precipitation in Gurbantunggut Desert, Central Asia." *Advances in Meteorology* 2015: 1–11. doi:[10.1155/2015/157245](https://doi.org/10.1155/2015/157245).
- Yang, Y. T., H. D. Guan, M. G. Shen, W. Liang, and L. Jiang. 2015b. "Changes in Autumn Vegetation Dormancy Onset Date and the Climate Controls across Temperate Ecosystems in China from 1982 to 2010." *Global Change Biology* 21 (2): 652–665. doi:[10.1111/gcb.12778](https://doi.org/10.1111/gcb.12778).
- Zang, H. J., X. Y. Li, J. Li, and J. Cai. 2011. "Response of Woody Plants' Spring Phenology to Climate Change in Shandong." *Chinese Journal of Agrometeorology* 32 (2): 167–173. doi: [10.3969/j.issn.1000-6362.2011.02.003](https://doi.org/10.3969/j.issn.1000-6362.2011.02.003)
- Zhang, X. S., Vegetation Map of China Editorial Committee, Chinese Academy of Sciences. 2007. *Vegetation Map of China and Its Geographic Pattern: Illustration of the Vegetation Map of the People's Republic China (1:10,000,000)*. 1–1. Beijing, China: Geographical Publishing House Press.
- Zhou, L., R. K. Kaufmann, Y. Tian, R. B. Myneni, and C. J. Tucker. 2003. "Relation between Interannual Variations in Satellite Measures of Northern Forest Greenness and Climate between 1982 and 1999." *Journal of Geophysical Research-Atmospheres* 108 (D1): 1–19. doi:[10.1029/2002JD002510](https://doi.org/10.1029/2002JD002510).
- Zhu, L. K., and J. J. Meng. 2015. "Determining the Relative Importance of Climatic Drivers on Spring Phenology in Grassland Ecosystems of Semi-Arid Areas." *International Journal of Biometeorology* 59 (2): 237–248. doi:[10.1007/s00484-014-0839-z](https://doi.org/10.1007/s00484-014-0839-z).